Selective Hydrogenation of Acetylene on TiO$_2$-Added Pd Catalysts

Jung Hwa Kang, Eun Woo Shin, Woo Jae Kim, Jae Duk Park, and Sang Heup Moon[1]

School of Chemical Engineering and Institute of Chemical Processes, Seoul National University,
San 56-1, Shillim-dong, Kwanak-ku, Seoul 151-744, Korea

The performance of TiO$_2$-modified Pd catalysts, containing TiO$_2$ either as an additive or as a support, in the selective hydrogenation of acetylene was investigated using a steady-state reaction test. The catalyst surface was characterized by H$_2$ and CO chemisorption, infrared, X-ray photoelectron spectroscopy (XPS), and the temperature-programmed desorption (TPD) of ethylene. The TiO$_2$-added Pd catalyst reduced at 500°C, denoted in this study Pd–Ti/SiO$_2$/500°C, showed a higher selectivity for ethylene production than either the Pd/TiO$_2$ or Pd/SiO$_2$ catalyst. The amounts of chemisorbed H$_2$ and CO were significantly reduced and, in particular, the adsorption of multiply coordinated CO species was suppressed on Pd–Ti/SiO$_2$/500°C, which is characteristic of the well-known strong-metal-support-interaction (SMSI) phenomenon that has been observed with the TiO$_2$-supported Pd catalyst reduced at 500°C, Pd/TiO$_2$/500°C. XPS analyses of Pd–Ti/SiO$_2$/500°C suggested an electronic modification of Pd by TiO$_2$, and the TPD of ethylene from the catalyst showed the weakening in ethylene adsorption on the Pd surface. 1,3-Butadiene was produced in smaller amounts when using Pd–Ti/SiO$_2$/500°C than when using Pd/SiO$_2$/500°C, indicating that the polymerization of C$_2$ species leading to catalyst deactivation proceeds at slower rates on the former catalyst than on the latter. The enhanced ethylene selectivity on Pd–Ti/SiO$_2$/500°C may be explained by correlating the catalyst surface properties with the mechanism of acetylene hydrogenation.

© 2002 Elsevier Science (USA)

Key Words: acetylene hydrogenation; ethylene selectivity; Pd; TiO$_2$; SMSI.

INTRODUCTION

The ethylene stream in a naphtha cracking unit contains a small quantity of acetylene, which is usually removed by selective hydrogenation over Pd-based catalysts (1). It has been reported that various additives, such as Ag, Ni, Cu, Pb, Tl, Cr, K, and Si (2–9), improve the performance of the Pd catalysts, particularly in achieving a high selectivity for ethylene production.

The role of the additives, or selectivity promoters, is generally considered to be derived from two factors: geometric

and electronic. For example, Leviness *et al.* (4) reported on ethylene-selectivity promotion by Cu, which they proposed to be due to a geometric effect. That is, the insertion of Cu into the Pd matrix decreases the number of multiple Pd sites responsible for the dissociative adsorption of acetylene and simultaneously suppresses the formation of β-phase Pd–hydride, both of which are detrimental to ethylene selectivity. Recently, Shin *et al.* (10) reported that the improved ethylene selectivity of Si-modified catalysts in acetylene hydrogenation is largely the result of the geometric dilution of the Pd surface with partially reduced SiO$_x$.

On the other hand, Huang *et al.* (2) observed an improved selectivity on Ag-promoted Pd catalysts, suggesting that an increase in the Pd d-band electron density by the addition of Ag was responsible for the enhanced selectivity. Boitiaux *et al.* (7) also reported that the enhanced performance of Pd–Cr catalysts in alkyne hydrogenation was derived from a change in the electronic properties of Pd by alloying with Cr.

In this study, we added TiO$_2$ to Pd catalysts as a potential selectivity promoter and investigated the performance of the TiO$_2$-added catalysts in acetylene hydrogenation. TiO$_2$ was selected as a candidate promoter because it is well-known that it interacts strongly with Pd, particularly after reduction at high temperatures. The phenomenon is referred to as "the strong metal-support interaction" (SMSI) and has been observed with catalysts supported on reducible metal oxides, including TiO$_2$ (11, 12).

The SMSI phenomenon is explained by the decoration of the metal surface with partially reduced metal oxides (13–18) or by an electron transfer between the support and the dispersed metals (19, 20). For example, Resasco and Haller (21) proposed a delocalized transfer of charge from Rh to TiO$_2$ on Rh/TiO$_2$ after a low-temperature reduction and a localized transfer of charge from the support to Rh after a high-temperature reduction. In addition, they proposed that the migration of a reduced species of the support onto the Rh surface following a high-temperature reduction is responsible, in part, for the decrease in the hydrogenolysis activity of Rh/TiO$_2$.

The analogy between the role of selectivity promoters of Pd catalysts in acetylene hydrogenation and the role of reducible oxide supports in the SMSI phenomenon prompted

us to examine the possibility of using TiO_2 as a promoter for the acetylene hydrogenation catalyst.

The goal of this study was twofold. First, we were interested in examining the surface properties of Pd catalyst containing TiO_2 as an additive instead of a support, and the other was to investigate the potential of using TiO_2 as a selectivity promoter of the Pd catalyst in acetylene hydrogenation.

We prepared Pd/SiO_2, Pd/TiO_2, and TiO_2-added Pd/SiO_2 catalysts, reduced them at different temperatures, and observed their performance in acetylene hydrogenation. The surfaces of catalysts were analyzed by using CO chemisorption, IR spectroscopy of the adsorbed CO (CO-IR), X-ray photoelectron spectroscopy (XPS), transmission electron microscopy (TEM), and the temperature-programmed desorption of ethylene (ethylene-TPD) and by monitoring the amounts of butadiene produced during the reaction.

EXPERIMENTAL

Catalyst Preparation

Pd/SiO_2 (1 wt%) and Pd/TiO_2 (1 wt%), which are denoted hereafter as Pd/SiO_2 and Pd/TiO_2, were prepared as reference catalysts using $Pd(NH_3)_4(NO_3)_2$ as a Pd precursor according to a method reported in the literature (22). Powders of silica (JRC-SIO-6 obtained from the Japanese Catalysis Society; surface area $= 109$ m^2/g) or titania (Degussa P25; surface area $= 50$ m^2/g) were added to a solution of $Pd(NH_3)_4(OH)_2$ obtained by contacting an aqueous solution of $Pd(NH_3)_4(NO_3)_2$ with an ion-exchange resin (Amberlite IRA 400 regenerated in KOH, 0.5 M). After stirring for 2 h, the suspension was centrifuged and washed with water. The catalyst was then dried at 110°C overnight and calcined in air at 300°C for 2 h.

The TiO_2-added Pd catalysts were prepared by impregnating Pd/SiO_2 with a hexane solution of diisopropoxide dipivaloylmethanato titanium $[Ti(O\text{-}i Pr)_2(DPM)_2; DPM =$ bis(2,2,6,6-tetramethyl-3,5-heptadionate, $C_{11}H_{19}O_2$)]. The catalysts are designated as Pd–xTi/SiO$_2$, with x denoting the Ti/Pd atomic ratio. For example, Pd–Ti represents Ti/Pd $= 1$ and Pd–10Ti represents Ti/Pd $= 10$. The catalyst samples were then calcined in air at 300°C for 3 h and reduced in H_2 at either 500 or 300°C for 1 h before use in the reaction.

H_2 and CO Chemisorption

Hydrogen uptake by the sample catalysts was measured at room temperature in a volumetric adsorption system. Prior to the measurements, the sample was reduced in a stream of H_2 at 300°C for 1 h, and the cell was then evacuated at the same temperature for 1 h. The amounts of hydrogen chemisorbed on the sample surface were determined by the backsorption method described by Benson et al. (23). In this procedure, the sample cell was evacuated

at room temperature for 20 min after the initial isotherm measurements, and then a second isotherm was obtained by introducing hydrogen into the cell.

The amounts of CO chemisorbed on the catalysts were measured at room temperature in a conventional glass vacuum system. The chemisorption cell, containing the sample catalyst, was evacuated at the catalyst-reduction temperature for 30 min and cooled to room temperature, and CO was then introduced into the cell for isotherm measurements. The CO pressure ranged between 10 and 150 Torr (1 Torr $= 133.3$ N m^{-2}).

CO-IR

All infrared spectra were collected using a MIDAC spectrometer (model 2100) equipped with a DTGS detector using an IR cell with CaF_2 windows, designed by Moon et al. (24). The catalyst, 40 mg, was pressed into a disk 18 mm in diameter and was placed in the sample holder located at the center of the cell. For CO-IR measurements, the catalyst was exposed to a 10-Torr pressure of CO for 5 min at 40°C. IR spectra were recorded at 5-min intervals during the initial 1-h period after the CO dosing, while the cell was evacuated.

XPS, TEM, and TPD

The chemical properties of the catalyst surface were examined with XPS (VG ESCA LAB-5) equipped with an Al $K\alpha$ (1486.6) anode. An electron gun was used to minimize surface charging. The electron-binding energies were calibrated by using the C 1s peak at 284.6 eV. The reduced catalyst samples were protected from air oxidation by wetting the surface with iso-octane (25), mounted on a double-sided adhesive tape, and then placed in a UHV chamber for XPS analysis. Catalysts were also analyzed with TEM (Philips, PECNINAI) for the estimation of their Pd particle size.

For the ethylene-TPD experiments, Pd/SiO_2 or Pd–Ti/SiO_2 was reduced in a microreactor for 1 h, cooled to room temperature, exposed to a mixture of ethylene and helium, and then flushed with helium to remove weakly adsorbed species from the catalyst surface. The TPD was performed by heating the sample from room temperature to 300°C at a rate of 10°C/min in a 20 cm^3/min flow of helium. The effluent gas was analyzed with a mass spectrometer (VG Sensorlab).

Acetylene Hydrogenation

Acetylene hydrogenation was performed in a pyrex microreactor at ambient pressure. A gas mixture containing 0.91% acetylene in ethylene was allowed to flow through a reactor which was maintained at 40°C and the reaction products were analyzed with an online gas chromatograph (H.P, model 5890 with FID) using a Porapak N column.

The H_2/acetylene ratio in the reactor feed was adjusted to 2 unless otherwise specified. The flow rate of the reactant mixture was varied between 40 and 120 cm^3/min to change the acetylene conversion. Ethylene selectivity was calculated as moles of ethylene produced per mole of acetylene converted.

$$S_{ethylene} = -\frac{\Delta C_2 H_4}{\Delta C_2 H_2}$$

RESULTS AND DISCUSSION

Gas Chemisorption, TEM, and CO-IR

Table 1 summarizes H_2 and CO adsorption data for the sample catalysts reduced at two different temperatures, 300 and 500°C, representing typical conditions for either inducing or not inducing the SMSI on Pd/TiO$_2$ (11, 12). For the case of Pd/SiO$_2$, the H/Pd and CO/Pd ratios are lowered by almost the same extent when the reduction temperature is raised from 300 to 500°C, which is apparently due to the sintering of Pd particles at 500°C. The Pd/TiO$_2$ catalyst reduced at 300°C, Pd/TiO$_2$/300°C, adsorbs smaller amounts of H_2 and CO than does Pd/SiO$_2$/300°C, suggesting that the Pd dispersion is relatively poor when TiO$_2$ instead of SiO$_2$ is used as a support. When Pd/TiO$_2$ is reduced at 500°C, Pd/TiO$_2$/500°C, gas adsorption is significantly reduced, which is the well-known SMSI phenomenon, as has been reported previously (11, 12).

The gas uptake by Pd–Ti/SiO$_2$/300°C, containing TiO$_2$ as an additive instead of a support, is slightly smaller than that by Pd/SiO$_2$/300°C, which probably occurs because TiO$_2$ covers the Pd surface or blocks the catalyst pores to some extent. The gas adsorption on Pd–Ti/SiO$_2$/500°C is suppressed similarly to the case of Pd/TiO$_2$/500°C, although the extent is not as large as in the latter.

To compare more directly the Pd dispersion of catalysts, we have obtained TEM pictures of the catalysts, either supported on or modified by TiO$_2$, after reduction at differ-

TABLE 1

H_2 and CO Adsorption Data for Sample Catalysts Reduced at Different Temperatures

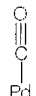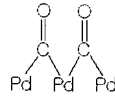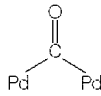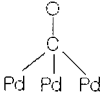| Catalysts	H/Pd	CO/Pd	A_m/A_l[a]	H/Pd[b]
Pd/SiO$_2$/300°C[c]	0.79	0.76	2.5	0.45
Pd/SiO$_2$/500°C	0.54	0.52	4.5	0.38
Pd/TiO$_2$/300°C	0.34	0.47	—	—
Pd/TiO$_2$/500°C	0.02	0.01	—	—
Pd–Ti/SiO$_2$/300°C	0.61	0.63	2.7	0.58
Pd–Ti/SiO$_2$/500°C	0.19	0.17	1.6	0.25

[a] The area ratio of the multiply bound to the linearly bound CO bands shown in Fig. 1.

[b] The H/Pd ratio for the catalyst oxidized in O_2 at 300°C and subsequently reduced at different temperatures.

[c] Pd/SiO$_2$ (1 wt%) reduced at 300°C.

TABLE 2

Assignments of IR Bands for CO Adsorbed on Pd[a]

Band	Wavenumber (cm^{-1})	Species
Linear	2100–2050	
Compressed bridged	1995–1975	
Isolated bridged	1960–1925	
Tricoordinated	1890–1870	

[a] Ref. (26).

ent temperatures. Although Fig. 1 shows limited portions of the catalysts, it is apparent that Pd particles are poorly dispersed on Pd/TiO$_2$/300°C compared with the case of Pd–Ti/SiO$_2$/300°C and that the particle size difference between the two catalysts is maintained even after reduction at 500°C.

To further study the surface properties of Pd–Ti/SiO$_2$, IR spectra of CO adsorbed on the catalyst were obtained and the results compared with those observed for Pd/SiO$_2$. The spectra shown in Fig. 2 represent four adsorption modes of CO (26), linear, compressed bridged, isolated bridged, and tricoordinated bonds, as described in Table 2. The bands for the multiply bound CO, including the bridged and tricoordinated types, are usually overlapped and characterized by peaks located below 2000 cm^{-1}.

On Pd/SiO$_2$, the overall intensity of the CO bands decreased and the area ratio of the multiply bound to the linearly bound bands, A_m/A_l, increased from 2.5 to 4.5 (Table 1) when the reduction temperature was raised from 300 to 500°C. This is in agreement with the CO chemisorption results in Table 1, suggesting the sintering of Pd particles after the reduction at 500°C. The CO band intensity on Pd–Ti/SiO$_2$/300°C is lower than that on Pd/SiO$_2$/300°C, again in agreement with the chemisorption results, indicating a partial coverage of the Pd surface with the Ti species. It should be noted that, in Fig. 1, the intensity of the 1870- to 1890-cm^{-1} band representing the tricoordinated CO adsorption is lowered as the result of TiO$_2$ addition, indicating that the Ti species preferentially blocks the sites with three adjacent Pd atoms.

The intensity of the CO bands on Pd–Ti/SiO$_2$ is significantly suppressed when the catalyst is reduced at 500°C, i.e., Pd–Ti/SiO$_2$/500°C. This result is not due to the sintering of Pd particles observed with Pd/SiO$_2$/500°C because, in this
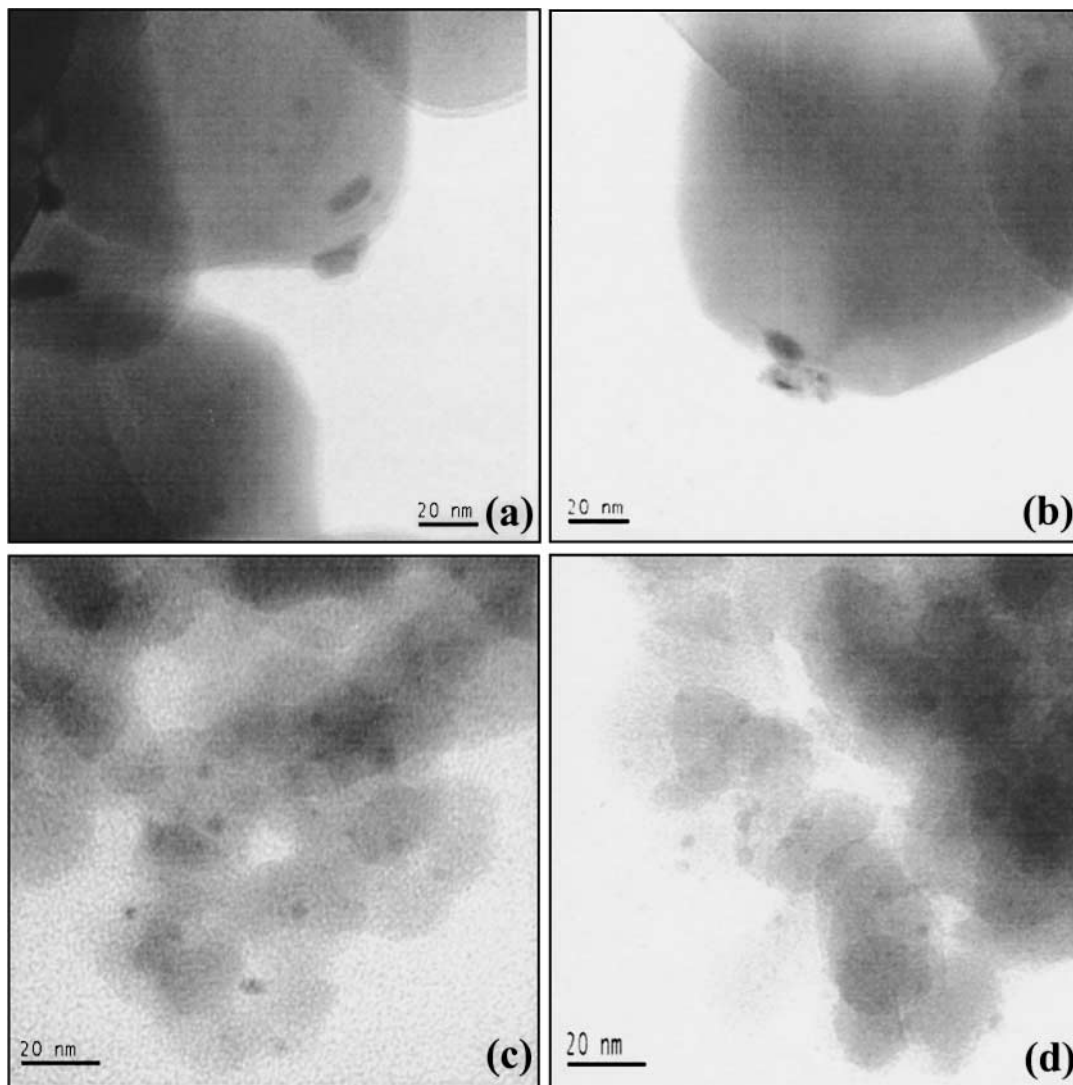
FIG. 1. TEM pictures of catalysts. (a) Pd/TiO$_2$/300°C, (b) Pd/TiO$_2$/500°C, (c) Pd–Ti/SiO$_2$/300°C, (d) Pd–Ti/SiO$_2$/500°C.

case, the area ratio, A_m/A_1, has decreased from 2.7 to 1.6 (Table 1), which is opposite the trend expected in the case of Pd sintering. The simultaneous suppression of the CO-band intensity and the A_m/A_1 ratio is possible when the Ti species added to the catalyst covers the Pd surface, thus blocking the multiply coordinated Pd sites, on Pd–Ti/SiO$_2$/500°C. In fact, this is the decoration model proposed for explaining the SMSI phenomenon that has been observed with TiO$_2$-supported catalysts (27, 28).

To obtain additional evidence for the SMSI phenomenon on Pd–Ti/SiO$_2$, we repeated the H$_2$ chemisorption and CO-IR observations after the initially reduced Pd–Ti/SiO$_2$ catalyst had been oxidized in O$_2$ at 300°C and subsequently reduced. Table 1 shows that the H/Pd ratio for the catalyst reduced at 300°C after oxidation, 0.58, is nearly the same as the initial value for Pd–Ti/SiO$_2$/300°C prior to oxidation, 0.61. When oxidized Pd–Ti/SiO$_2$ is reduced at 500°C a

second time, the H/Pd ratio becomes 0.25, close to the initial value, 0.19. The above reversible behavior of gas adsorption on Pd–Ti/SiO$_2$ after oxidation-reduction treatments, which is characteristic of the SMSI phenomenon (11, 12), is also observed for the CO-IR results shown in Fig. 3. That is, the spectra of CO adsorbed on the catalysts after the oxidation-reduction treatments are similar to those obtained prior to the oxidation step, except for a minor difference in the spectral shape, which is possibly due to Pd sintering during the treatments.

Unlike Pd–Ti/SiO$_2$, Pd/SiO$_2$ does not show reversible behavior for gas adsorption. In Table 1, the H/Pd ratio for Pd/SiO$_2$/500°C, 0.54, is lowered to 0.45 when the catalyst is reduced at 300°C after oxidation and is further lowered to 0.38 after a subsequent reduction at 500°C. These results for Pd/SiO$_2$ merely reflect the sintering of Pd particles during the oxidation and reduction steps.
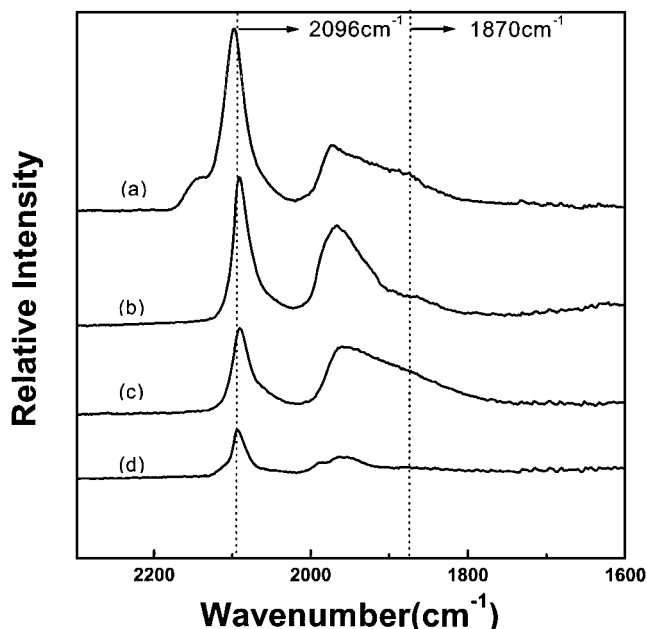
FIG. 2. Infrared spectra of CO adsorbed on sample catalysts. (a) Pd/SiO$_2$/300°C, (b) Pd–Ti/SiO$_2$/300°C, (c) Pd/SiO$_2$/500°C, (d) Pd–Ti/SiO$_2$/500°C.

From the above results, we conclude that the SMSI phenomenon observed with the TiO$_2$-supported catalyst, Pd/TiO$_2$/500°C, is also observed with the TiO$_2$-added catalyst, Pd–Ti/SiO$_2$/500°C. It can be argued that there is
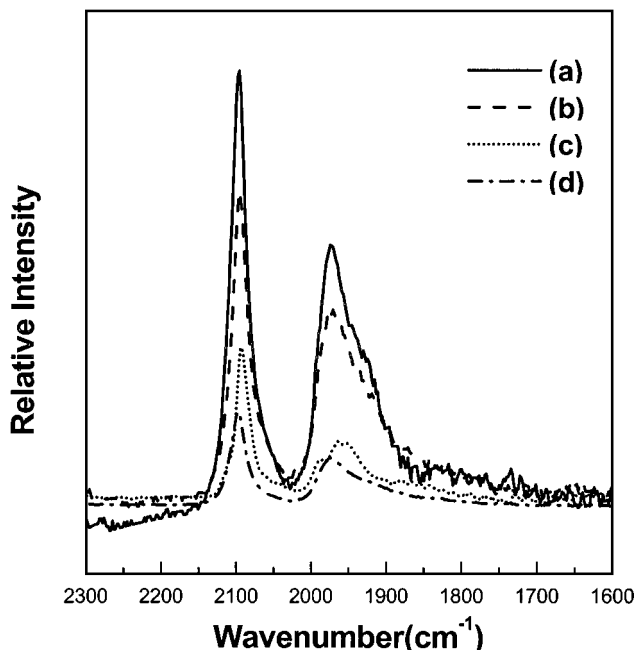

FIG. 3. Infrared spectra of CO adsorbed on sample catalysts reduced prior to or after the oxidation treatment. (a) Pd–Ti/SiO$_2$/300°C (prior to oxidation), (b) Pd–Ti/SiO$_2$/300°C (after oxidation), (c) Pd–Ti/SiO$_2$/500°C (after oxidation), (d) Pd–Ti/SiO$_2$/500°C (prior to oxidation).

TABLE 3

Typical Acetylene Conversions Obtained Using Sample Catalysts under Identical Reaction Conditions

Catalysts	Conversion[a]
Pd/SiO$_2$/300°C[b]	0.72
Pd/SiO$_2$/500°C	0.56
Pd/TiO$_2$/300°C	0.54
Pd/TiO$_2$/500°C	0.28
Pd–Ti/SiO$_2$/300°C	0.64
Pd–Ti/SiO$_2$/500°C	0.35

[a] Reaction condition: temperature = 40°C; H$_2$/acetylene = 2; space velocity = 1000/h.
[b] Pd/SiO$_2$ (1 wt%) reduced at 300°C.

no advantage to adding TiO$_2$ to Pd/SiO$_2$ over supporting Pd on TiO$_2$ because the catalysts prepared by both methods contain TiO$_2$ and exhibit the same SMSI phenomenon. However, a clear advantage of using TiO$_2$ as an additive instead of a support is that highly dispersed Pd catalysts can be obtained by this method. The difference in the Pd dispersion between the TiO$_2$-added and TiO$_2$-supported catalysts is maintained even after reduction at 500°C, as indicated in Fig. 1.

Catalytic Performance

Table 3 lists typical acetylene conversion data obtained using the catalysts prepared in this study under identical reaction conditions. The conversion obtained using Pd/SiO$_2$/500°C is lower than for Pd/SiO$_2$/300°C because Pd particles are sintered during the reduction at 500°C, as explained in the previous section. Pd/TiO$_2$/300°C shows a lower conversion than Pd/SiO$_2$/300°C because Pd dispersion is relatively poor on the TiO$_2$ support. Pd/TiO$_2$ loses its activity even further after reduction at 500°C because the Pd surface is decorated with a large amount of Ti species, a distinctive feature of the SMSI phenomenon (27, 28). The TiO$_2$-added catalyst, Pd–Ti/SiO$_2$, also suffers a loss in activity after reduction at 500°C, but the activity loss is smaller than that in the case of Pd/TiO$_2$.

It should be noted, however, that the activity losses of the TiO$_2$-containing catalysts, Pd/TiO$_2$ and Pd–Ti/SiO$_2$, after reduction at 500°C are not as great as would be expected from their chemisorption results, the latter showing a significant suppression of H$_2$ uptake. In fact, a similar discrepancy between gas uptake and catalyst activity was observed when the SMSI catalysts were used for CO hydrogenation, which has not been completely explained to date (29, 30). We believe that a large fraction of the catalyst surface exhibiting the SMSI phenomenon continues to be available for acetylene hydrogenation, although the surface is capable of accommodating only small amounts of adsorbed H$_2$ and CO. We have not attempted to estimate the turnover
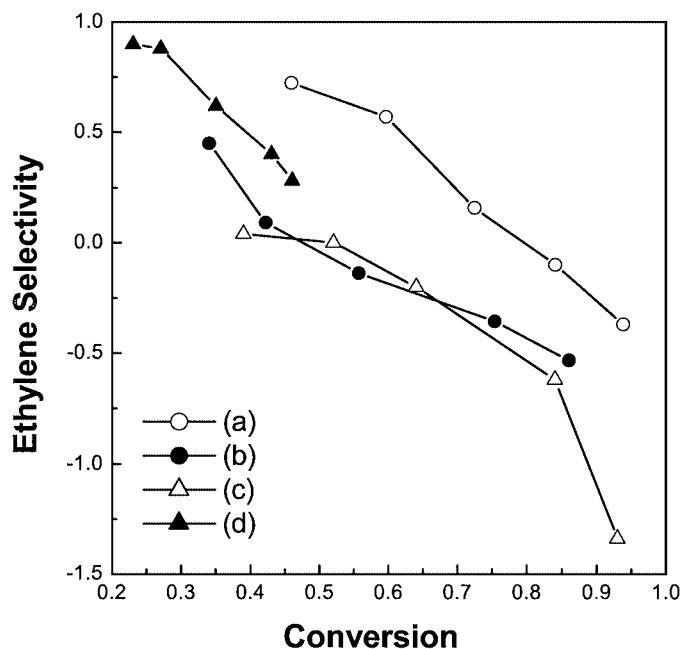
FIG. 4. Changes in ethylene selectivity with conversion in acetylene hydrogenation on sample catalysts supported on different supports (H_2/acetylene $= 2$, $T = 40°C$). (a) Pd/SiO$_2$/300°C, (b) Pd/SiO$_2$/500°C, (c) Pd/TiO$_2$/300°C, (d) Pd/TiO$_2$/500°C.

frequencies of the catalysts in acetylene hydrogenation due to the uncertainty of the size of the Pd surface area of the TiO$_2$-containing catalysts.

The activity data in Table 3 indicate that TiO$_2$, whether used as an additive or as a support, is not an activity promoter of a Pd catalyst in acetylene hydrogenation. On the other hand, TiO$_2$ is useful as a promoter of ethylene selectivity in acetylene hydrogenation, as described below.

Since ethylene is produced as an intermediate in acetylene hydrogenation, which is a typical consecutive reaction, the ethylene selectivity decreases with acetylene conversion, as shown in Fig. 4. The selectivity becomes negative for a few catalysts particularly at high conversions, indicating a net loss of ethylene by the reaction. Figure 4 shows that the selectivity is lower on Pd/SiO$_2$/500°C than on Pd/SiO$_2$/300°C, which occurs because the former catalyst contains larger Pd particles than the latter. It has been reported that ethylene selectivity is lower on the low-index Pd surface, e.g., Pd(100), than on the high-index surface, e.g., Pd(111) (31).

The selectivity curve for Pd/TiO$_2$/300°C nearly overlaps that for Pd/SiO$_2$/500°C. However, the curve for Pd/TiO$_2$/500°C is shifted upward to some extent, suggesting that the selectivity may be improved when the catalyst exhibits the SMSI phenomenon. Nevertheless, the performance of Pd/TiO$_2$/500°C is still inferior to that of Pd/SiO$_2$/300°C, in terms of both selectivity and conversion, because of the poor dispersion of Pd particles in the TiO$_2$-supported catalyst.

Figure 5A shows the selectivity curves for TiO$_2$-added catalysts, Pd–Ti/SiO$_2$. It should be noted that the selectivity is always higher for Pd–Ti/SiO$_2$/300°C than for Pd/SiO$_2$/300°C over a wide range of conversions. The selectivity curve is shifted upward when the catalyst is reduced at 500°C, Pd–Ti/SiO$_2$/500°C, which clearly demonstrates the beneficial role of TiO$_2$ as a selectivity promoter. We believe
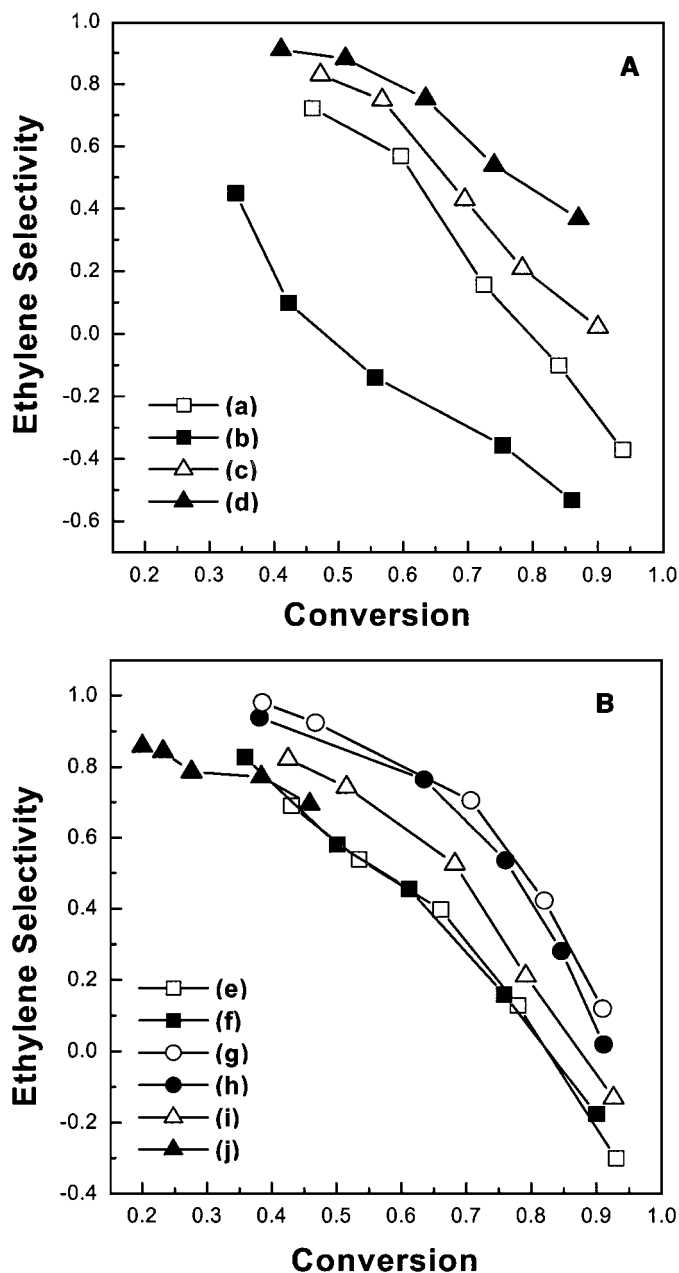

FIG. 5. Changes in ethylene selectivity with conversion in acetylene hydrogenation on catalysts containing different amounts of TiO$_2$. A: (a) Pd/SiO$_2$/300°C, (b) Pd/SiO$_2$/500°C, (c) Pd–Ti/SiO$_2$/300°C, (d) Pd–Ti/SiO$_2$/500°C. B: (e) Pd/SiO$_2$/300°C, (f) Pd–0.5Ti/SiO$_2$/500°C, (g) Pd–Ti/SiO$_2$/500°C, (h) Pd–2Ti/SiO$_2$/500°C, (i) Pd–4Ti/SiO$_2$/500°C, (j) Pd–10Ti/SiO$_2$/500°C.

that the above good performance of the Pd–Ti/SiO$_2$ catalyst is achieved because of the addition of TiO$_2$ to the well-dispersed Pd/SiO$_2$ catalyst; with Pd/TiO$_2$, performance is limited by the poor dispersion of Pd on TiO$_2$.

Different amounts of TiO$_2$ were added to Pd/SiO$_2$ and the performance of the catalysts were observed, as shown in Fig. 5B. Selectivity is promoted by the addition of TiO$_2$ but is eventually retarded when the Ti/Pd ratio is higher than 4.0. In Fig. 5B, Pd–10Ti/SiO$_2$/500°C shows low conversions and the selectivity is nearly the same as that for Pd/SiO$_2$/300°C, apparently because a large portion of the Pd surface is covered with Ti species. The maximum selectivity is obtained when the Ti/Pd ratio falls between 1.0 and 2.0.

To determine if this is due to a unique property of the Ti precursor used in the catalyst preparation, we prepared a set of Pd–Ti/SiO$_2$ catalysts using different Ti precursors and examined their catalytic behaviors. Figure 6 indicates that the selectivity-conversion relation is relatively unaffected by the Ti precursors when the catalysts are reduced under identical conditions. We therefore conclude that the selectivity promotion by TiO$_2$ is the result of an intrinsic interaction between the Pd surface and the Ti species, which is largely affected by the TiO$_2$ content and the reduction temperature.

FIG. 7. XPS of Pd 3d$_{5/2}$ for sample catalysts. (a) Pd/SiO$_2$/300°C, (b) Pd–Ti/SiO$_2$/300°C, (c) Pd–Ti/SiO$_2$/500°C, (d) Pd–10Ti/SiO$_2$/500°C.

XPS and TPD

To understand the origin of the selectivity promotion by the Ti species, we observed the XPS of the catalysts. Figure 7 shows that the peak representing the binding energy of Pd 3d$_{5/2}$ appears almost at the same position for Pd/SiO$_2$/300°C and Pd–Ti/SiO$_2$/300°C but is shifted to lower binding energy for Pd–Ti/SiO$_2$/500°C. The peak shift is larger for Pd–10Ti/SiO$_2$/500°C. The spectra are free from possible charging effects because the XPS (VG ESCA LAB-5) used in this study for the measurements is equipped with an electron shower gun to minimize the charging effect and, furthermore, the observed peak positions have been adjusted in reference to the C 1s peak.

The shift in metal binding energy, as measured by XPS, is influenced not only by the electronic interaction of the metal with other components but also by the size of metal crystallites. For example, Takasu *et al.* (32) observed in their study of Pd particles which were deposited on SiO$_2$ that the binding energy of Pd 3d$_{5/2}$ decreased by 1.6 eV when the Pd particle size increased within a range smaller than 5 nm. Similar trends have been reported for Ag and Pt particles (33, 34).

Based on the H/Pd ratio data given in Table 1, the average Pd particle sizes of Pd/SiO$_2$/300°C and Pd/SiO$_2$/500°C are estimated to be 23 and 33 Å, respectively, which fall within the range exhibiting the binding energy change as a function of the Pd particle size, according to Takasu *et al.* (32). Because the TiO$_2$-containing catalyst would be expected to have Pd particle size similar to that of the Pd/SiO$_2$ catalyst when the reduction temperature is the same, the
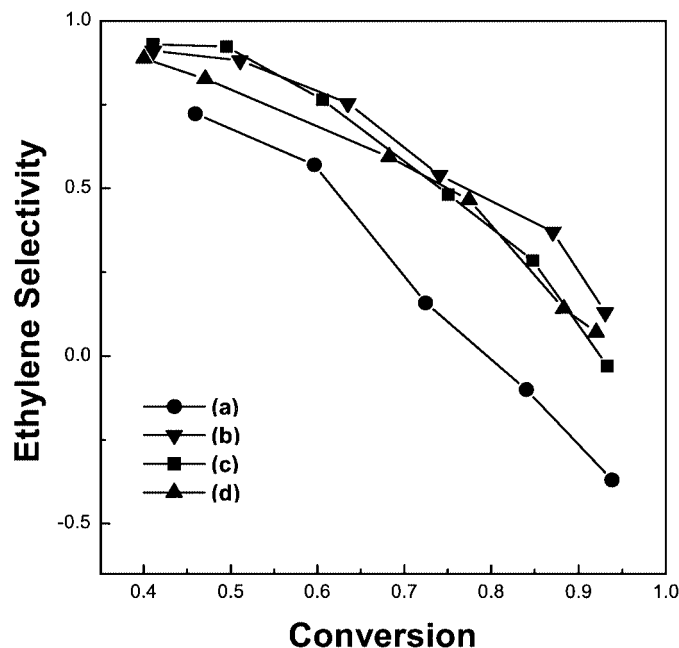

FIG. 6. Changes in ethylene selectivity with conversion in acetylene hydrogenation on sample catalysts prepared from different Ti sources (H$_2$/acetylene = 2, T = 40°C). (a) Pd/SiO$_2$/300°C, (b) Pd–Ti/SiO$_2$/500°C [Ti source = titanium acetylacetonate, Ti(acac)$_2$], (c) Pd–Ti/SiO$_2$/500°C [Ti source = diisopropoxide dipivaloylmethanato titanium, Ti(O-iPr)$_2$ (DPM)$_2$], (d) Pd–Ti/SiO$_2$/500°C [Ti source = tetrabutoxyl titanium, Ti(O-Bu)$_4$].
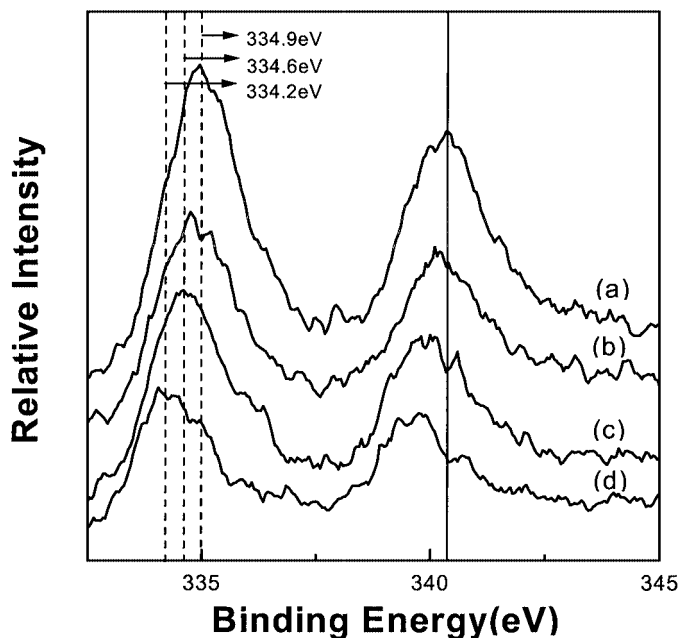
XPS peak shifts observed with Pd–Ti/SiO$_2$/500°C and Pd–10Ti/SiO$_2$/500°C, shown in Fig. 7, may represent a particle-size effect. In other words, the peak is shifted to lower binding energy because Pd particles grow after reduction at 500°C.

However, the above interpretation does not explain the large peak shift observed for Pd–10Ti/SiO$_2$/500°C because the shift should be to the same extent as that for Pd–Ti/SiO$_2$/500°C if it is solely dependent on Pd particle size. Accordingly, the possibility of electronic modification of Pd by TiO$_2$ cannot be completely excluded and, in fact, has been observed in many studies of the SMSI effect (35–37). For example, negative XPS peak shifts on the order of 0.2 to 1.6 eV were reported for Ni/TiO$_2$ (38), Pt/TiO$_2$ (39), and Pt/SrTiO$_3$ (40) after these catalysts had been reduced at temperatures higher than 500°C. Lee *et al.* (41) observed that the binding energy of Pd $3d_{5/2}$ decreased from 335.2 to 334.8 eV on the addition of ZrO$_2$ to Pd supported on α-Al$_2$O$_3$. Chien *et al.* (42) reported that the binding energy shift on Rh/TiO$_2$ resulted from the transfer of a negative charge to Rh particles from Ti^{3+}, which is formed by the reduction of TiO$_2$.

The XPS results also allow us to estimate the relative concentrations of Ti and Pd on the catalyst surface, as listed in Table 4. The Ti/Pd ratio for the Pd–Ti/SiO$_2$ catalyst increases when the reduction temperature is raised from 300 to 500°C, suggesting that the Pd surface is covered with larger fractions of the Ti species after reduction at 500°C. The Ti/Pd ratio is significantly large for Pd–10Ti/SiO$_2$/500°C, which contains an excess amount of Ti species.

The peaks of ethylene-TPD from the Pd surface appear at different temperature ranges depending on the characteristic modes of the ethylene adsorbed on the surface. In Fig. 8, Pd/SiO$_2$/300°C shows two major peaks, which may be assigned as follows, based on the analysis by Stuve and Madix (43), although the peak locations are different between the two studies because they were made under different experimental conditions. The peak centered at 54°C is assigned to π-bonded ethylene, which is weakly adsorbed and consequently desorbed without decomposition. The peak at 125°C is due to di-σ-bonded ethylene, which undergoes de-
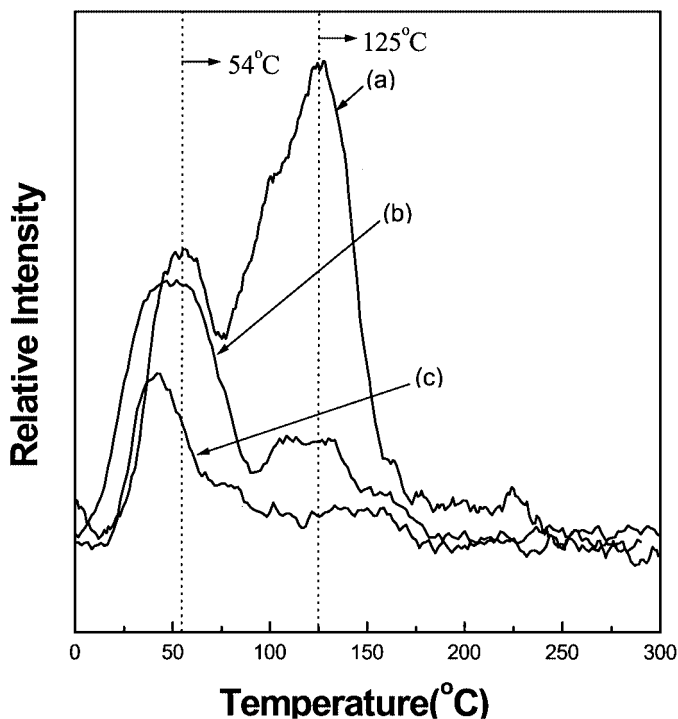

FIG. 8. TPD of ethylene from sample catalysts. (a) Pd/SiO$_2$/300°C, (b) Pd–Ti/SiO$_2$/300°C, (c) Pd–Ti/SiO$_2$/500°C.

composition followed by the recombination of the surface hydrocarbon species with hydrogen to produce ethylene as well as ethane. In the case of Pd–Ti/SiO$_2$/300°C, the peak at 125°C is significantly reduced and the low temperature peak is slightly shifted to lower temperatures. The trend is greater for Pd–Ti/SiO$_2$/500°C, i.e., the peak at 125°C has nearly disappeared and the low-temperature peak of reduced intensity is shifted even further.

The ethylene-TPD results are in agreement with the IR and XPS results in the following aspects. The Pd surface is modified geometrically by the Ti species, as evidenced by the CO-IR spectra, such that the decomposition of ethylene is suppressed. The charge transfer from the Ti species to Pd weakens the adsorption strength of ethylene, e.g., ethylidene, on the Pd surface such that the species is desorbed at lower temperatures. In fact, the TPD results in this study are consistent with those previously reported by Briggs *et al.* (44), who also observed a reduction in the strength of ethylene adsorption on Pt/TiO$_2$, which had been reduced at elevated temperatures. They attributed the weakening of the adsorption strength to interactions between Pt and partially reduced titania.

Investigation of 1,3-Butadiene Formation

1,3-Butadiene, which is produced by the dimerization of C$_2$ species, is known as a precursor of the green oil, which accumulates on the catalyst surface (45). Butadiene is produced particularly when acetylene is adsorbed on

TABLE 4

The Ti/Pd Ratios Estimated from XPS Results for Sample Catalysts

Catalysts	Pd $(3d_{5/2})$	Peak intensity ratio Ti$_{2p}$/Pd$_{3d}$
Pd/SiO$_2$/300°C	334.9	—
Pd–Ti/SiO$_2$/300°C	334.9	1.16
Pd–Ti/SiO$_2$/500°C	334.6	1.61
Pd–10Ti/SiO$_2$/500°C	334.2	11.11

neighboring Pd sites and is not readily hydrogenated on the catalyst surface. Once butadiene is formed, it undergoes polymerization, eventually leading to catalyst fouling. Accordingly, an analysis of the butadiene content in the product stream of acetylene hydrogenation is one of the methods used to monitor catalyst deactivation.

Figure 9 shows the concentration of 1,3-butadiene observed in the exit stream of the reactor containing either Pd/SiO$_2$/300°C or Pd–Ti/SiO$_2$/500°C. The butadiene concentration has been plotted against the accumulated amount of acetylene converted in the process instead of the reaction period, so that the catalysts can be compared on the basis of the same reaction load. Figure 9 indicates that butadiene is produced in smaller amounts on Pd–Ti/SiO$_2$/500°C than on Pd/SiO$_2$/300°C. Because the formation of 1,3-butadiene requires multiple sites of Pd to accommodate adjacent C$_2$ species, the above result suggests that large ensembles of Pd are blocked by the Ti species, thus suppressing the formation of green oil.

To verify a parallel relationship between the butadiene concentration in the product stream and the catalyst deactivation rate, we performed time-on-stream experiments while monitoring changes in the catalyst activity with time. Figure 10 shows conversions normalized to the initial value for Pd/SiO$_2$/300°C and Pd–Ti/SiO$_2$/500°C versus the accumulated amount of converted acetylene, which allows us to compare the catalyst aging behaviors for the same load of acetylene hydrogenation. It is obvious from Fig. 10 that Pd–Ti/SiO$_2$/500°C undergoes slower deactivation than
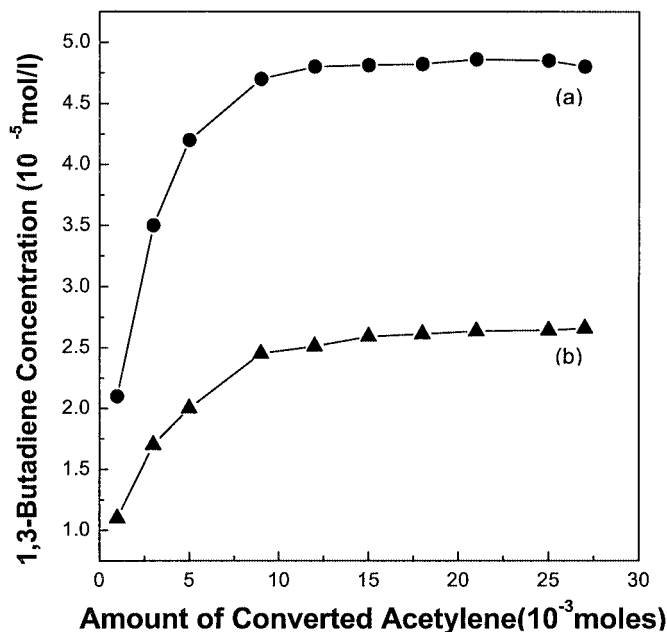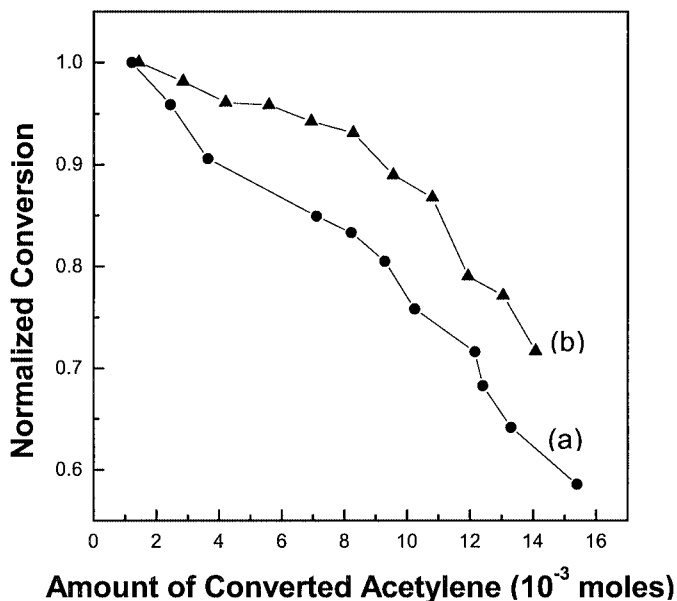

FIG. 10. Changes in the normalized conversion with the accumulated amount of converted acetylene (H$_2$/acetylene $= 1$, $T = 70$°C). (a) Pd/SiO$_2$/300°C, (b) Pd–Ti/SiO$_2$/500°C.

Pd/SiO$_2$/300°C, as expected from the butadiene formation results.

Origin of the Selectivity Promotion

The findings herein show that ethylene selectivity is higher on Pd–Ti/SiO$_2$/500°C than on Pd/SiO$_2$/300°C over a range of acetylene conversions. To understand the origin of the selectivity improvement particularly on the TiO$_2$-added catalyst, it is necessary to consider the reaction mechanism for acetylene hydrogenation, which comprises several reaction paths, as shown in Fig. 11 (4, 46–48). Path I represents the partial hydrogenation of acetylene to ethylene, which is subsequently desorbed to the desired gaseous product (Path II) or further hydrogenated to ethane on the catalyst surface (Path III). Obviously, Path II should be promoted and Path III suppressed to improve ethylene selectivity, for which two methods are typically used in industrial processes. One is to add a moderator chemical to the reaction stream, e.g., CO, which adsorbs more strongly on Pd than ethylene and, consequently, replaces ethylene on the catalyst surface (49). The other is to maintain a low H$_2$/acetylene ratio in the feed such that the catalyst surface is low in hydrogen concentration (47, 48). Path IV, representing the direct full hydrogenation of acetylene to ethane, is insignificant at high acetylene coverage and low partial pressures of hydrogen (50), which is the case in most industrial processes. The triply adsorbed species, ethylidyne, had been proposed as an intermediate in Path IV (4, 31, 50, 51) but was later verified to be a simple spectator of surface reactions (52, 53). Path V, which allows for the dimerization
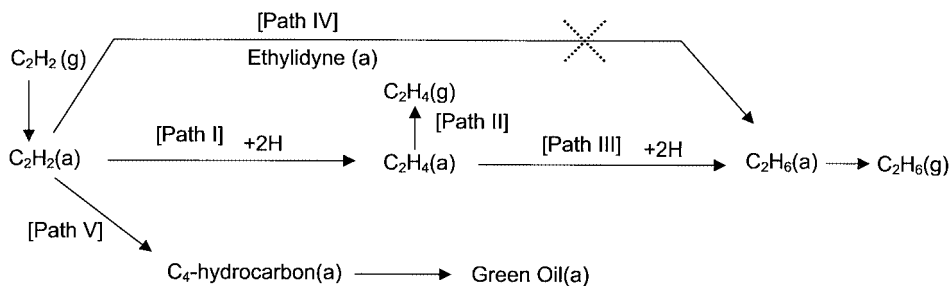

FIG. 9. The concentration of 1,3-butadiene measured in the exit stream of reactor containing sample catalysts (H$_2$/acetylene $= 1$, $T = 70$°C). (a) Pd/SiO$_2$/300°C, (b) Pd–Ti/SiO$_2$/500°C.

FIG. 11. Reaction paths of acetylene hydrogenation.

of the C_2 species, eventually leads to catalyst deactivation via the accumulation of green oil (54, 55). Path V lowers the ethylene selectivity because it consumes acetylene but does not produce ethylene. Accordingly, the mechanism of acetylene hydrogenation indicates that, for improving ethylene selectivity, Paths I and II should be promoted while the other paths should be suppressed.

In this study, we have obtained the following properties for TiO$_2$-added catalyst, particularly for Pd–Ti/SiO$_2$/500°C.

1. Small Pd crystallites on the Pd/SiO$_2$ catalyst are preserved even after TiO$_2$ addition and reduction at 500°C, although the Pd surface is decorated with Ti species to different extents depending on the reduction temperatures.

2. H$_2$ adsorption is significantly suppressed, the origin of which is the same SMSI phenomenon as observed for the TiO$_2$-supported catalysts.

3. Ethylene adsorption is suppressed in two ways. The ethylene decomposition is inhibited because the multiple Pd sites are blocked by Ti species, and the adsorption of ethylene is weakened presumably because Pd is electronically modified by the Ti species.

4. 1,3-Butadiene is produced in smaller amounts than in the case of Pd/SiO$_2$, suggesting that the polymerization of the C$_2$ species proceeds at slower rates on the TiO$_2$-added catalyst.

The above properties of Pd–Ti/SiO$_2$/500°C are correlated with the reaction paths for acetylene hydrogenation such that the selectivity improvement of the catalyst may be explained based on either the promotion or the suppression of individual paths.

Small Pd crystallites are advantageous for the suppression of Path V because they have small fractions of the low-index Pd surface, which is responsible for the dimerization of the C$_2$ species. Path V is further suppressed when the Pd surface is decorated with, and consequently the neighboring Pd sites are blocked by, Ti species. This explanation is consistent with the observation that 1,3-butadiene is produced in smaller amounts on Pd–Ti/SiO$_2$/500°C than on Pd/SiO$_2$/300°C.

The significant suppression of H$_2$ adsorption on Pd–Ti/SiO$_2$/500°C will suppress both Paths I and III. In fact,

this situation is the same as using low H$_2$/acetylene ratios in the feed of acetylene hydrogenation, which suppresses Path III more than Path I and consequently improves ethylene selectivity (47, 48).

The inhibition of the triply bound species, ethylidyne, on Pd–Ti/SiO$_2$/500°C will suppress Path IV, although its contribution to selectivity is insignificant. On the other hand, the weakening of ethylene adsorption on Pd–Ti/SiO$_2$/500°C obviously contributes to the ethylene selectivity because it promotes Path II, leading to the production of gaseous ethylene.

Accordingly, the surface properties of Pd–Ti/SiO$_2$/500°C agree with the trends the reaction paths of acetylene hydrogenation would be expected to follow to allow for the ethylene selectivity promotion.

CONCLUSIONS

In this study, we demonstrated that TiO$_2$-added Pd catalyst reduced at 500°C, Pd–Ti/SiO$_2$/500°C, shows the same SMSI phenomenon as is observed for Pd/TiO$_2$, containing TiO$_2$ as a support. Pd–Ti/SiO$_2$/500°C shows an improved selectivity for ethylene production in acetylene hydrogenation compared with the case of Pd/SiO$_2$/300°C, which may be explained based on the correlation between the surface properties of the catalyst and the reaction paths for acetylene hydrogenation. Pd–Ti/SiO$_2$/500°C is advantageous over either Pd/SiO$_2$/500°C or Pd/TiO$_2$/500°C catalysts because it shows a higher Pd dispersion, and accordingly a higher hydrogenation activity, than the latter catalysts in addition to the promotion in the ethylene selectivity.

REFERENCES

1. Lam, W. K., and Lloyd, L., *Oil Gas J*. **27**, 66 (1972).
2. Huang, D. C., Chang, K. H., Pong, W. F., Tseng, P. K., Hung, K. J., and Hung, W. F., *Catal. Lett*. **53**, 155 (1998).

3. Miegge, P., Rousset, J. L., Tardy, B., Massardier, J., and Bertolini, J. C., *J. Catal.* **149**, 404 (1994); doi: 10.1006/jcat.1994.1307.

4. Leviness, S., Nair, V., Weiss, A. H., Schay, Z., and Guczi, L., *J. Mol. Catal.* **25**, 131 (1984).

5. Sandoval, V. H., and Gigola, C. E., *Appl. Catal. A* **148**, 81 (1996).

6. Cerveny, L., Paseka, I., Surma, K., Thanh, N. T., and Ruzicka, V., *Collect. Czech. Chem. Commun.* **50**, 61 (1985).

7. Boitiaux, J. P., Cosyns, J., Derrien, M., and Leger, G., *Hydrocarbon Process.*, March, 51 (1985).

8. Park, Y. H., and Price, G. L., *Ind. Eng. Chem. Res.* **31**, 469 (1992).

9. Shin, E. W., Choi, C. H., Chang, K. S., Na, Y. H., and Moon, S. H., *Catal. Today* **44**, 137 (1998).

10. Shin, E. W., Kang, J. H., Kim, W. J., Park, J. D., and Moon, S. H., *Appl. Catal. A* **223**, 161 (2002).

11. Tauster, S. J., and Fung, S. C., *J. Catal.* **55**, 29 (1978).

12. Tauster, S. J., Fung, S. C., and Garten, R. L., *J. Am. Chem. Soc.* **100**, 170 (1978).

13. Santos, J., Phillips, J., and Dumesic, J. A., *J. Catal.* **81**, 147 (1983).

14. Sadeghi, H. R., and Henrich, V. E., *J. Catal.* **87**, 279 (1984).

15. Simoens, A. J., Baker, R. T. K., Dwyer, D. J., Lund, C. R. F., and Madon, R. J., *J. Catal.* **86**, 359 (1984).

16. Chung, Y.-W., Xiong, G., and Kao, C. C., *J. Catal.* **85**, 237 (1984).

17. Ko, C. S., and Gorte, R. J., *J. Catal.* **90**, 59 (1984).

18. Raupp, G. B., and Dumesic, J. A., *J. Catal.* **95**, 587 (1985).

19. Herrmann, J. M., Gravelle-Rumeau-Maillot, M., and Gravelle, P. C., *J. Catal.* **104**, 136 (1987).

20. Chou, P., and Vannice, M. A., *J. Catal.* **104**, 1 (1987).

21. Resasco, D. E., and Haller, G. L., *J. Catal.* **82**, 279 (1983).

22. Liotta, L. F., Deganello, G., Delichere, P., Leclercq, C., and Matin, G. A., *J. Catal.* **164**, 334 (1996); doi: 10.1006/jcat.1996.0389.

23. Benson, J. E., Hwang, H. S., and Boudart, M., *J. Catal.* **30**, 146 (1973).

24. Moon, S. H., Windawi, H., and Katzer, J. R., *Ind. Eng. Chem. Fundam.* **20**, 396 (1981).

25. Arteaga, A., Fierro, J. L. G., Delanny, F., and Delmon, B., *Appl. Catal.* **26**, 227 (1986).

26. Tessier, D., Rakai, A., and Verduraz, B., *J. Chem. Soc. Faraday Trans.* **88**, 741 (1992).

27. Simoens, A. J., Baker, R. T. K., Dwyer, D. J., Lund, C. R. F., and Madon, R. J., *J. Catal.* **86**, 359 (1984).

28. Spencer, M. S., *J. Catal.* **93**, 216 (1985).

29. Stevenson, S. A., Dumesic, J. A., Baker, R. T. K., and Ruckenstein, E., *in* "Metal-Support Interaction in Catalysis, Sintering and Redispersion." van Nostrand Reinhold, New York, 1987.

30. Haller, G. L., and Resasco, D. E., *Adv. Catal.* **36**, 173 (1991).

31. Sarkany, A., Weiss, A. H., and Guczi, L., *J. Catal.* **98**, 550 (1986).

32. Takasu, Y., Unwin, R., Tesche, B., and Bradshaw, A. M., *Surf. Sci.* **77**, 219 (1978).

33. Mason, M. G., Gerenser, L. J., and Lee, S.-T., *Phys. Rev. Lett.* **39**, 288 (1977).

34. Mason, M. G., and Baetzold, R. C., *J. Chem. Phys.* **64**, 271 (1976).

35. Mériaudeau, P., Ellestad, O. H., and Naccache, C., *J. Catal.* **75**, 243 (1982).

36. Chen, B.-H., and White, J. M., *J. Phys. Chem.* **86**, 3534 (1982).

37. Matsuda, S., and Kato, A., *Appl. Catal.* **8**, 149 (1983).

38. Bahl, M. K., Tsai, S. C., and Chung, Y. W., *Phys. Rev. B* **21**, 1344 (1980).

39. Fung, S. C., *J. Catal.* **76**, 225 (1982).

40. Kao, C. C., Tsai, S. C., Bahl, M. K., Chung, Y. W., and Lo, W. J., *Surf. Sci.* **95**, 1 (1980).

41. Lee, Y., Inoue, Y., and Yasumori, I., *Bull. Chem. Soc. Jpn.* **54**, 3711 (1981).

42. Chien, S. H., Shelimov, B. N., Resasco, D. E., Lee, E. H., and Haller, G. L., *J. Catal.* **77**, 301 (1982).

43. Stuve, E. M., and Madix, R. J., *J. Phys. Chem.* **89**, 105 (1985).

44. Briggs, D., Dewing, J., Burden, A. G., Moyes, R. B., and Wells, P. B., *J. Catal.* **65**, 31 (1980).

45. Margitfalvi, J., Guczi, L., and Weiss, A. H., *React. Kinet. Catal. Lett.* **15**, 475 (1980).

46. Zhang, Q., Li, J., Liu, X., and Zhu, Q., *Appl. Catal. A* **197**, 221 (2000).

47. Duca, D., Frusteri, F., Parmaliana, A., and Deganello, G., *Appl. Catal. A* **146**, 269 (1996).

48. Derrien, M. L., *Stud. Surf. Sci. Catal.* **27**, 613 (1986).

49. Park, Y. H., and Price, G. L., *Ind. Eng. Chem. Res.* **30**, 1693 (1991).

50. Margitfalvi, J., Guczi, L., and Weiss, A. H., *J. Catal.* **72**, 185 (1981).

51. Moses, J. M., Weiss, A. H., Matusek, K., and Guczi, L., *J. Catal.* **86**, 417 (1984).

52. Backman, A. L., and Masel, R. I., *J. Vac. Sci. Technol. A* **9**, 1789 (1991).

53. Beebe, T. P., Jr., Albert M. R., and Yates, J. T., Jr., *J. Am. Chem. Soc.* **108**, 663 (1986).

54. Larsson, M., Jansson, J., and Asplund, S., *J. Catal.* **178**, 49 (1998).

55. Battiston, G. C., Dalloro, L., and Tauszik, G. R., *Appl. Catal.* **2**, 1 (1982).